

Spectral modeling (0.5-2.5 μm) of the Phobos Blue-Red transition area

Maurizio Pajola (1), Ted Roush (2), Cristina Dalle Ore (2,3), Giuseppe A. Marzo (4) and Emanuele Simioni (1)
(1) INAF, Osservatorio Astronomico di Padova, Vicolo dell'Osservatorio 5, 35122, Padova, Italy (maurizio.pajola@oapd.inaf.it), (2) NASA Ames Research Center, Moffett Field, CA, 94035, USA, (3) Carl Sagan Center, SETI Institute, Mountain View, CA, 94043, USA, (4) ENEA C. R. Casaccia, 00123, Roma, Italy

Abstract

We here focus on the spectral modeling of the surface of Phobos in the wavelength range between 0.5 and 2.5 μm exploiting the Phobos Mars Reconnaissance Orbiter/Compact Reconnaissance Imaging Spectrometer for Mars (MRO/CRISM) dataset obtained on 2007 October 23. The spatial scale of this dataset is 355 m/pixel, while the phase angle of the observation is $\sim 37.5^\circ$ [1]. The CRISM observation covers the sub-Mars hemisphere of Phobos, from Stickney crater's interior and rim, to the limit between the leading and trailing hemispheres of the satellite (Fig. 1A). This area is of particular interest because it is the most variegated region on Phobos and it has different spectral slopes in the Vis/NIR wavelength range. The fresher areas close to Stickney crater have a lower color ratio, and are the "Blue unit" of [2], Fig. 1B. This unit is considered as the fresh ejecta deposit excavated from the interior of Phobos and resulting from the oblique impact that generated Stickney. Instead, the background areas are characterized by a higher ratio and are the "Red unit" of [3].

Without a priori selecting specific surface locations, we include spectra from nearly the entire surface observed. We use the unsupervised K-means partitioning algorithm developed by [4] in order to investigate the spectral variability across Phobos' surface. This technique has been extensively validated using spectral data sets and applied to Mars [4-6], Iapetus [7,8], Charon [9] and Mercury [10]. After correcting the CRISM data to a standard viewing geometry (using incidence and emission maps to minimize the influence of local topography on the spectra), the statistical partitioning identifies seven clusters over the observed surface of Phobos (Fig. 1C). From these clusters we eliminate both cluster 0, that corresponds to the space around Phobos and those associated to the limb/terminator of

the satellite (clusters no. 1 and 2), and then investigate the compositional information contained within the average spectra of the remaining four clusters by using the radiative transfer model of [11].

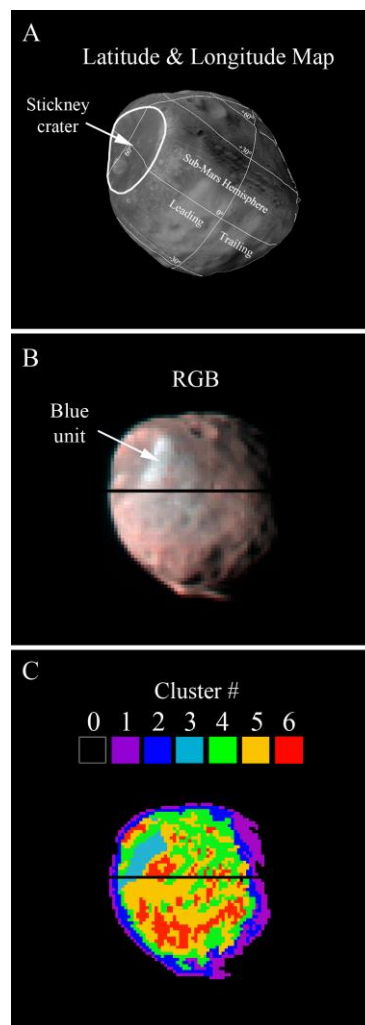


Fig. 1: A) The Phobos area observed by CRISM. B) RGB image from CRISM Vis region (R=0.90 μm , G=0.58 μm , B=0.50 μm). C) The seven clusters identified on Phobos.

As previously suggested by [12], we use the optical constants of Tagish Lake meteorite (TL, [13]), and pyroxene glass (PM80, [14,15]) as inputs for the calculations. The results show a good slope agreement when compared to the averages of the CRISM spectral clusters (Fig. 2). In particular, the best fitting model of the cluster with the steepest spectral slope (cluster no. 6) yields relative abundances that are equal to those of [12], i.e. 20% PM80 and 80% TL, but grain sizes that are slightly different with respect to [12].

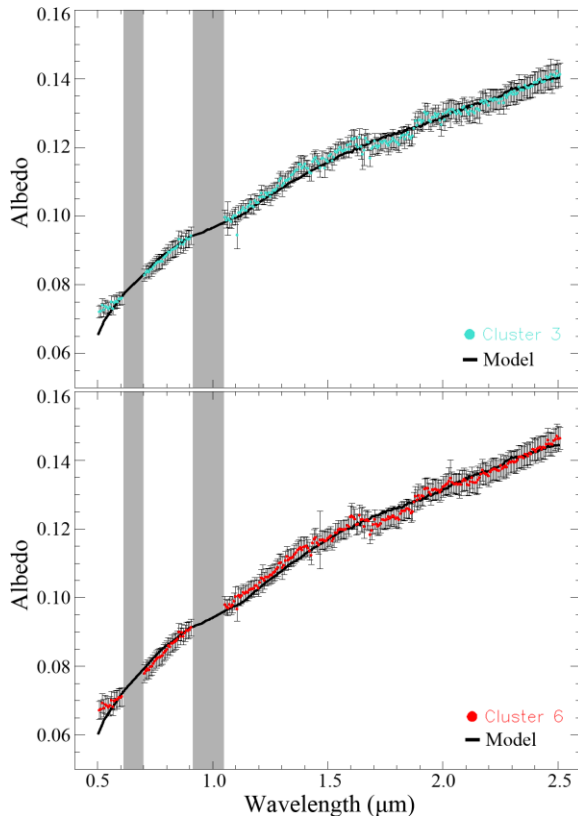


Fig. 2: The spectra of clusters 3 and 6 with the corresponding models. The bars associated correspond to the 1σ values. The grey bars indicate the CRISM bad bands not considered in the modeling.

Such discrepancy may arise from the fact that the areas observed in this work and those analyzed in [12] are on opposite locations on Phobos and present different morphological and weathering settings. On the contrary, as the clusters spectral slopes decrease, the best fits obtained show trends related to both relative abundance and grain size that is not observed for the cluster with the steepest spectral slope. With a decrease in slope there is general increase of relative percentage of PM80 from 12% to 18% and the

associated decrease of TL from 88% to 82%. Simultaneously the PM80 grain sizes decrease from 9 to 5 μm and TL grain sizes increase from 13 to 16 μm .

The best fitting models show relative abundances and grain sizes that partially overlap. This supports the hypothesis that from a compositional perspective the transition between the highest and lowest slopes on Phobos is subtle, and it is characterized by a smooth change of relative abundances and grain sizes, rather than a distinct dichotomy between the areas.

Acknowledgements

M.P. was supported for this research by an appointment to the NASA Postdoctoral Program at the Ames Research Center, administered by Universities Space Research Association (USRA) through a contract with NASA. The NASA PDS Archive node is acknowledged for providing access to the CRISM dataset used in this work.

References

- [1] Pajola, M. et al., 2018. *Planet. Space Sci.* 154, 63-71.
- [2] Murchie, S., Erard, S., 1996. *Icarus* 123, 63.
- [3] Murchie, S., et al., 1999. *J. Geophys. Res.* 104, 9069–9080.
- [4] Marzo, G., et al., 2006. *J. Geophys. Res.* 111. E03002.
- [5] Marzo, G., et al., 2008. *J. Geophys. Res.* 113. E12009.
- [6] Fonti, S., Marzo, G.A., 2010. *Astron. Astrophys.* 512 (A51), 6 pp.
- [7] Pinilla-Alonso, N., et al., 2011. *Icarus* 215 (1), 75.
- [8] Dalle Ore, C., et al., 2012. *Icarus* 221 (2), 735.
- [9] Dalle Ore, C., et al., 2018. *Icarus* 300, 21–32.
- [10] Lucchetti, et al., 2017. *48 Lunar and Planetary Science Conference*, 1964.
- [11] Shkuratov, Y., et al., 1999. *Icarus* 137, 235.
- [12] Pajola, M., et al., 2013. *Astrophys. J.* 777, 127, 6 pp.
- [13] Roush, T.L., 2003. *M&PS* 38, 419.
- [14] Jaeger, C., et al. 1994. *Astron. Astrophys.* 292, p. 641.
- [15] Dorschner, J., et al. 1995. *Astron. Astrophys.* 300, p. 503.